

# High-resolution Brillouin light scattering and angle-dependent 9.4-GHz ferromagnetic resonance in MBE-grown Fe/Cr/Fe on GaAs

S. M. Rezende, M. A. Lucena, F. M. de Aguiar, A. Azevedo, and C. Chesman  
*Departamento de Física, Universidade Federal de Pernambuco, 50670-901 Recife, Brazil*

P. Kabos and C. E. Patton  
*Department of Physics, Colorado State University, Ft. Collins, Colorado 80523*

(Received 26 August 1996)

Exploiting the high sensitivity of a recently assembled Brillouin-light-scattering (BLS) spectrometer, we investigate the magnetic excitations with nonvanishing in-plane wave vector  $\mathbf{k}$  in antiferromagnetically coupled Fe/Cr/Fe (001), grown by molecular-beam epitaxy. The BLS spectra reveal surprisingly rich structures not previously observed in this very sample. In addition, we use angle-dependent 9.4-GHz ferromagnetic resonance to probe the uniform ( $k=0$ ) collective excitation, previously investigated at 35 GHz. The observation of the acoustic and optical modes by both techniques allowed the determination of an accurate set of material parameters from the fit of theoretical curves to all data. While the results do not invalidate earlier conclusions, we offer an updated model which provides an alternative explanation for the observed spectra without the assumption of an extra effective surface anisotropy field. [S0163-1829(97)00513-4]

## I. INTRODUCTION

Ultrathin multiple films of a ferromagnetic metal with intervening films of a nonmagnetic material have enjoyed a great deal of interest in recent years. On certain circumstances, such films exhibit remarkable magnetoresistive effects<sup>1</sup> which have been investigated in detail by the magnetic-recording industry. These effects are connected with an antiferromagnetic alignment of the magnetizations of adjacent magnetic layers in these artificial structures.<sup>2</sup> The Fe/Cr/Fe system is probably the most explored in this regard. In addition to the basic discoveries reported in Refs. 1 and 2, subsequent experimental findings include oscillatory magnetoresistance and interlayer exchange coupling as a function of the Cr thickness,<sup>3</sup> shorter period oscillations,<sup>4</sup> oscillations as a function of the Fe thickness<sup>5</sup> and an intriguing 90-deg coupling of the Fe films.<sup>6,7</sup> All these findings have been either predicted or followed by a number of proposed mechanisms which represent subjects of current investigations.

In this work we revisit the Brillouin-light-scattering (BLS) experiments in a well exercised Fe/Cr/Fe sandwich structure grown by molecular-beam epitaxy (MBE), whose dynamic magnetic response was originally investigated by ferromagnetic resonance<sup>8</sup> (FMR) and later by BLS.<sup>9</sup> Rich spectra have been observed at various frequencies with the FMR technique<sup>8</sup> but, for unknown reasons, a full analysis of the optical response was not possible since only a single mode was observed in the previous BLS experiments.<sup>9</sup> Here we explore the higher sensitivity of a recently assembled BLS spectrometer and show that the richness of the FMR results<sup>8</sup> can indeed be matched by the BLS technique. In addition, we use angle-dependent 9.4-GHz FMR to independently determine the magnetic anisotropy and effective magnetization of this sample. Angle-dependent FMR has been previously explored only at 35 GHz in the multiple-frequency experiments of Ref. 8. In contrast with the results of Ref. 9, we demonstrate that quantitative fits to the experi-

mental data can be obtained without the use of an effective surface anisotropy field, provided one takes into account a higher-order term in the approximation to the effective dipolar field.

## II. THEORETICAL CONSIDERATIONS

As mentioned above, the sample under consideration was grown by MBE and characterized at the Naval Research Laboratory.<sup>8</sup> It consists of an epitaxial (100) Fe(38 Å)/Cr(13 Å)/Fe(38 Å) thin-film sandwich grown onto (100) GaAs substrate coated with a 2000-Å-thick ZnSe buffer layer. Symmetry and protection of the top iron layer were provided by a 1000-Å-thick (100) ZnSe overcoat layer. As previously reported,<sup>8,9</sup> the overall magnetic behavior of this sample is complicated. The static and dynamic responses result from a competition of three main interactions, namely, the exchange coupling between the iron layers, the magnetocrystalline anisotropy within a layer, and the coupling between the layers magnetizations with the external magnetic field. The interlayer exchange interaction is weakly antiferromagnetic. The film also exhibits a small amount of uniaxial anisotropy along *one* in-plane [110] direction, in addition to the usual cubic anisotropy of (100) Fe. In general, each of these interactions tries to align the magnetizations of the two iron layers in different ways. Our first goal is to characterize the equilibrium position of the magnetizations as a function of the applied magnetic field. This procedure is necessary for a reliable interpretation of the excitation spectra, since there is a close relationship between the static configuration and the dynamic response of the system. In the following, we present an overview of our model calculations. Details of this analysis will be published separately.

Let  $\mathbf{M}_1$  and  $\mathbf{M}_2$  be the magnetizations in the iron films of thicknesses  $d_1$  and  $d_2$ , respectively. The coordinate system used to characterize these vectors and the applied in-plane magnetic  $\mathbf{H}$  is shown in the inset of Fig. 1(a). The sample

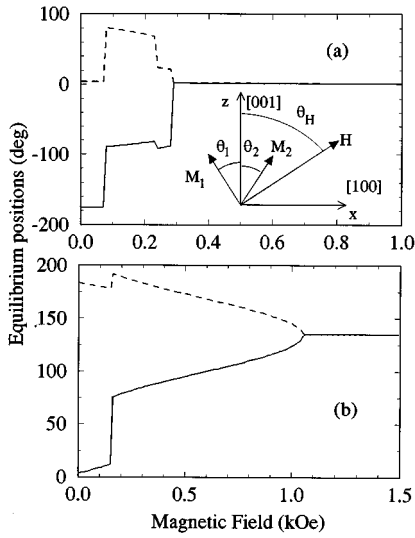


FIG. 1. Calculated equilibrium positions of the magnetizations in the two iron films,  $\theta_1$  (solid line) and  $\theta_2$  (dashed line), as a function of the applied magnetic field  $H$ , with (a)  $\mathbf{H} \parallel [001]$  and (b)  $\mathbf{H} \parallel [10\bar{1}]$ . Parameters are given in the text. The inset shows the coordinate system used in the calculations.

surface lies in the  $xz$  plane and each direction considered below is characterized by an angle with respect to the  $z$  axis. Both  $x$  and  $z$  axes are taken to be along easy-magnetization directions. The uniaxial anisotropy direction  $[10\bar{1}]$  bisects the  $xz$  plane at  $\theta_U = 135^\circ$ . For each value of the field angle  $\theta_H$ , the equilibrium directions of  $\mathbf{M}_1$  and  $\mathbf{M}_2$  are found by minimizing the free energy. This is done numerically by varying the angles of  $\mathbf{M}_1$  and  $\mathbf{M}_2$ , respectively,  $\theta_1$  and  $\theta_2$ , first in steps of  $5^\circ$  to locate the range of minimum energy, and then in steps of  $0.5^\circ$  to obtain accurate equilibrium conditions. The free energy per unit area contains contributions due to Zeeman, cubic anisotropy, the uniaxial in-plane anisotropy, and the interlayer exchange-coupling energies. Typical results are shown in Fig. 1 for two field directions, namely,  $\theta_H = 0$  [Fig. 1(a)] and  $\theta_H = 135^\circ$  [Fig. 1(b)]. The curves are based on a magnetic layer saturation magnetization term  $4\pi M_s$  of 19.0 kG, a cubic anisotropy field  $H_A$  of 0.52 kOe, an in-plane uniaxial anisotropy field  $H_U$  of 0.070 kOe, an antiferromagnetic interlayer exchange field  $H_1$  of  $-0.12$  kOe, a thicknesses ratio  $d_1/d_2$  of 1.08, and a  $g$  factor of 2.12. These parameters are only slightly different from those used in Refs. 8 and 9 and were chosen on the basis of theoretical fits to the BLS and FMR data to be described in the next section. These differences produce no appreciable change in the fits to magnetization data. As already described in Refs. 8 and 9, Fig. 1(a) shows four distinct regions when  $\theta_H = 0$  is satisfied. These regions are separated by sudden discontinuous jumps of  $\mathbf{M}_1$  and  $\mathbf{M}_2$ . As shown in Fig. 1(b), the number of different regions is reduced to three when the field is applied along the  $[10\bar{1}]$  direction at  $\theta_H = 135^\circ$ . In this case, the second transition at  $H \approx 1.05$  kOe is less abrupt and there is no jump, so that one might observe in a single field sweep first- and second-order-like transitions in the magnetizations configuration. As mentioned before, the agreement with previous analysis is essentially retained. The

key results come about when the dynamic response of the system is considered.

Since the magnetizations in each field region have different configurations, the dynamic excitation frequencies are expected to behave differently as well. The frequencies measured by FMR and BLS correspond to the same basic type of magnetic excitation. The FMR technique probes excitations with wave number  $k$  close to zero, whereas the BLS probes modes with a nonvanishing in-plane  $k$  value, which is determined by the experimental scattering configuration. These frequencies have been calculated from the linearized torque equation,

$$\frac{d\mathbf{M}_n}{dt} = \gamma \mathbf{M}_n \times \mathbf{H}_n, \quad (1)$$

in the limit of small deviations of  $\mathbf{M}_n$  from equilibrium. Here  $\mathbf{H}_n$ , the effective field acting on magnetization  $\mathbf{M}_n$  ( $n=1,2$ ), can be described by the sum  $\mathbf{H}_n = \sum_I \mathbf{H}_{In}$ , where  $\mathbf{H}_{In}$  is the effective field associated with the corresponding interaction energy  $E_I$ . For the interlayer exchange coupling, the uniaxial and cubic anisotropies, and the Zeeman energies, the corresponding effective field is determined through the relation  $\mathbf{H}_{In} = \partial E_I / \partial \mathbf{M}_n$ . In order to give a full account for the dynamical response of the system, however, we have to consider other interactions as well. First, the intralayer ferromagnetic exchange interaction in the Fe films, which introduces the well-known quadratic dependence of the spin-wave excitation frequencies on wave number, is particularly important in the interpretation of the BLS spectra. Second, the dipole-dipole interaction between the two magnetic films, which, as usual, is taken into account in the magnetostatic approximation  $\nabla \times \mathbf{H}_{\text{DIP}} \approx 0$ , allowing one to use a magnetic scalar potential  $\Phi$  such that the effective dipolar field  $\mathbf{H}_{\text{DIP}} = -\nabla \Phi$ . The assumption of small deviations of the film magnetization from equilibrium results in a Poisson equation for the scalar potential,  $\nabla^2 \Phi = 4\pi \nabla \cdot \mathbf{M}$ . Following Cochran and coworkers,<sup>10</sup> the dipolar field components resulting from the solution of this standard boundary-value problem can be expanded in the small parameters  $ky$  and  $kd_n$ . The authors in Ref. 10 keep only the first-order terms and, as a result, terms linear in  $y$  are neglected, since their torque average to zero when integrated across the film. Alternatively, we integrate the effective field exactly over  $y$  in the averaging process,<sup>11</sup> keeping the next higher-order terms in  $kd_n$ . Altogether, we further reduce the resulting set of six coupled equations to a system of only four equations by choosing independent and convenient coordinate systems for each film.<sup>11</sup> This system of four equations is then numerically solved for the excitation frequencies  $\omega$ . As shown below, this approach provides quantitative agreement with the BLS and FMR measurements without the inclusion of an additional surface anisotropy.<sup>9</sup> The incorporation of an extra effective surface anisotropy field is somewhat disturbing since it introduces a sort of ambiguity in regard to the effective saturation magnetization value that must fit consistently both BLS and FMR spectra. This outstanding issue seems to have not as yet been settled and our alternative approach might be seen as an attempt to remove this defect.

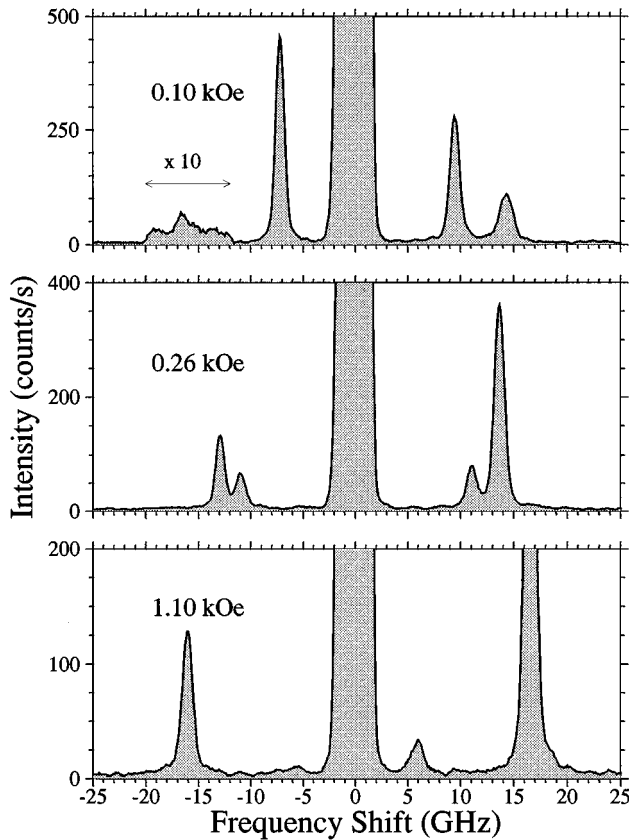


FIG. 2. Measured BLS spectra in the Fe(38 Å)/Cr(13 Å)/Fe(38 Å) film for three different values of the applied field  $\mathbf{H} \parallel [10\bar{1}]$ .

### III. EXPERIMENTAL RESULTS AND ANALYSIS

The BLS measurements were carried out in the back-scattering geometry, using a Sandercock tandem Fabry-Pérot (FP) interferometer in a  $(2 \times 3)$ -pass configuration. The light source was a single-mode-stabilized argon-ion laser operating at 5145 Å, with incident power of 70 mW. The sample for these measurements, with dimensions  $4 \times 1 \text{ mm}^2$ , was mounted between the poles of an electromagnet so that it could be rotated around the normal to the film plane as well as around the applied field direction, the latter being parallel to the film plane and perpendicular to the incidence plane of the light beam. The measurements were done at room temperature with an incidence angle of  $35^\circ$ , corresponding to a scattering in-plane spin-wave wave number  $k \sim 1.48 \times 10^5 \text{ cm}^{-1}$  and to an expansion parameter  $kd \sim 0.056$ . The collimated light beam at the output of the FP interferometer was focused on a 40% quantum efficiency solid-state photodetector (EG&G, model SPCM-200) with a dark count below 2 counts/s, connected to a multichannel card in a personal computer. With such a system, we were able to observe the missing optical mode in addition to the previously investigated acoustic mode,<sup>9</sup> typically within 5–10 min scans for each spectrum. Since the case in which the applied field is parallel to an easy-magnetization  $[100]$  axis was investigated in some detail, while only qualitative agreement was found for the  $[10\bar{1}]$  hard direction,<sup>9</sup> we will consider here only the situation with  $\theta_H = 135^\circ$ . In Fig. 2 we show three representative spectra for  $H = 0.10, 0.26,$  and  $1.10 \text{ kOe}$ . The measured dispersion relation is shown by the circles (optical

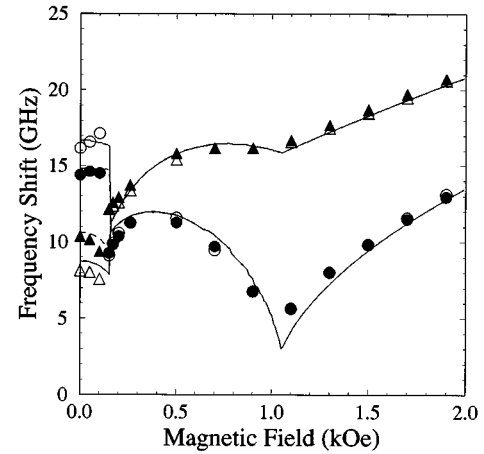


FIG. 3. BLS spin-wave dispersion relation observed in Fe(38 Å)/Cr(13 Å)/Fe(38 Å) with  $\mathbf{H} \parallel [10\bar{1}]$ , showing the behavior of the optical (circles) and acoustic (triangles) modes as a function of the applied field. Solid and dashed lines are results of numerical simulations of the corresponding Stokes (open symbols) and anti-Stokes (solid symbols) lines, respectively. The asymmetry below 0.15 kOe is a signature of the antiferromagnetic configuration of the magnetizations in the two Fe films.

mode) and triangles (acoustic mode) in Fig. 3, the Stokes and anti-Stokes lines being distinguished by the corresponding solid and open symbols, respectively. We note that the results in Fig. 3 correlate quite well with the calculated equilibrium configurations shown in Fig. 1(b). In the low-field region,  $0 < H < H_1 \approx 0.15 \text{ kOe}$ , where the magnetizations are aligned antiparallel, the spectra are remarkably asymmetric, in good quantitative agreement with the theoretical results [solid (Stokes) and dashed (anti-Stokes) lines in Fig. 3]. As

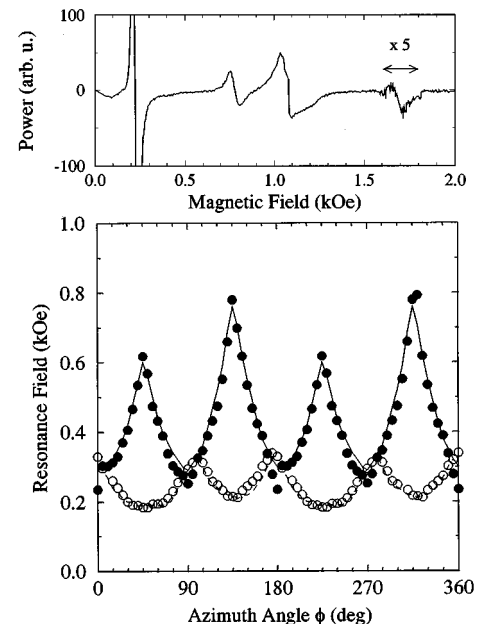


FIG. 4. Upper panel: Measured FMR spectrum at 9.4 GHz with  $\mathbf{H} \parallel [10\bar{1}]$ . Lower panel: Measured angle-dependent FMR resonance fields of the acoustic (open circles) and optical (solid circles) modes. The corresponding dashed and solid lines are results of numerical simulations as described in the text.

the magnetizations abruptly enter the spin-flop phase at  $H=H_1$ , there is a sudden squeeze of the spin-wave frequencies followed by an inversion of the modes positions, and the asymmetry is no longer present at higher field values. The dispersion relation exhibits butterfly-shaped curves for both modes for  $H>H_1$ , with cusp and local minima frequencies at the saturation field  $H_2\approx 1.05$  kOe.

The room-temperature angle-dependent FMR measurements were performed at 9.4 GHz by monitoring the derivative of the absorption line for a TE<sub>102</sub> rectangular microwave cavity with  $Q=2500$ . The sample was located at the center of the cavity and could be externally rotated around the normal to the film plane. This setup differs from the one used in Ref. 8 where the sample formed a shorting plate at the end of a coaxial line. As shown in the following, the overall behavior of this sample has been preserved. In Fig. 4(a), for instance, we show the FMR spectrum with the in-plane field  $\mathbf{H} \parallel [10\bar{1}]$ . As in the previous 35 GHz measurements,<sup>8</sup> it was possible to observe several resonance lines at 9.4 GHz. We concentrate on the two strongest lines, which correspond to the symmetric (acoustic) and antisymmetric (optical) precession modes.<sup>12</sup> The other peaks correspond to the same precession modes, whose curves  $\omega$  vs  $H$  cross the line  $\omega/2\pi=9.4$  GHz at different values of  $H$ . The dependence of the in-plane resonance fields on the azimuthal angular position  $\phi$  with respect to  $\mathbf{H}$  is shown in Fig. 4(b) [solid (optical mode) and open (acoustic mode) circles] along with the corresponding theoretical fits [solid (optical mode) and dashed (acoustic mode) lines].

We emphasize that the remarkable quantitative agreement

of the theory with both BLS and FMR spectra shown in Figs. 3 and 4 was obtained with the same set of phenomenological parameters with no assumption of an extra surface anisotropy field.<sup>9</sup> Besides the ones already mentioned, the only additional parameter used to fit the dynamical response, and which is relevant only to the BLS experiments, is the intralayer exchange stiffness  $D=2.0\times 10^{-9}$  Oe cm<sup>2</sup>/rad<sup>2</sup>, since the interlayer dipolar field is expressed in terms of other geometric and magnetic parameters already used. The simultaneous quantitative fits to the FMR and BLS data, the later being achieved here at last for both  $[001]$  and  $[10\bar{1}]$  directions, might be indicative that the smallness of  $kd\sim 0.056$  is only apparent and, thus, that higher-order approximations to the dipolar field could play an important role. We leave this provocative issue as a challenge for forthcoming works in this field.

### ACKNOWLEDGMENTS

Dr. G. A. Prinz and Dr. J. J. Krebs of the Naval Research Laboratories, Washington D.C., are acknowledged for kindly providing the Fe/Cr/Fe thin film used in this work, and for helpful comments and discussions on the results. The work at UFPE has been supported by CNPq, CAPES, PADCT, FINEP, and FACEPE (Brazilian agencies). The work at CSU was supported in part by the National Science Foundation under Grant No. DMR-9400276, U.S. Office of Naval Research under Grant No. N00014-94-0096 and by the U.S. Army Research Office under grants No. DAAL03-91-G0327 and DAAH04-95-1-0325.

<sup>1</sup>M. N. Baibich, J. M. Broto, A. Fert, F. Nguyen Van Dau, F. Petroff, P. Etienne, G. Creuzet, A. Freiderichs, and J. Chazelas, *Phys. Rev. Lett.* **61**, 2472 (1988).

<sup>2</sup>P. Grünberg, S. Schreiber, Y. Pang, M. B. Brodsky, and H. Sowers, *Phys. Rev. Lett.* **57**, 2442 (1986).

<sup>3</sup>S. S. P. Parkin, N. More, and K. Roche, *Phys. Rev. Lett.* **64**, 2304 (1990).

<sup>4</sup>S. T. Purcell, W. Folkerts, M. T. Johnson, N. W. E. McGee, K. Jager, J. aan de Stegge, W. B. Zeper, W. Hoving, and P. Grünberg, *Phys. Rev. Lett.* **67**, 903 (1991).

<sup>5</sup>S. N. Okuno and K. Inomata, *Phys. Rev. Lett.* **72**, 1553 (1994).

<sup>6</sup>A. Schreyer, J. F. Ankner, Th. Zeidler, H. Zabel, C. F. Majkrzak,

M. Schäfer, and P. Grünberg, *Europhys. Lett.* **32**, 595 (1995).

<sup>7</sup>A. Azevedo, C. Chesman, S. M. Rezende, F. M. de Aguiar, X. Bian, and S. S. P. Parkin, *Phys. Rev. Lett.* **76**, 4837 (1996).

<sup>8</sup>J. J. Krebs, P. Lubitz, A. Chaiken, and G. A. Prinz, *Phys. Rev. Lett.* **63**, 1645 (1989); *J. Appl. Phys.* **67**, 5920 (1990).

<sup>9</sup>P. Kabos, C. E. Patton, M. O. Dima, and D. B. Church, *J. Appl. Phys.* **75**, 3553 (1994).

<sup>10</sup>J. F. Cochran, J. Rudd, W. B. Muir, B. Heinrich, and Z. Celinski, *Phys. Rev. B* **42**, 508 (1990).

<sup>11</sup>R. L. Stamps, *Phys. Rev. B* **49**, 339 (1994).

<sup>12</sup>S. M. Rezende and F. M. de Aguiar, *Phys. Lett. A* **208**, 286 (1995); *J. Appl. Phys.* **79**, 6309 (1996).